Low-frequency hippocampal–cortical activity drives brain-wide resting-state functional MRI connectivity

Russell W. Chan[a,b,1], Alex T. L. Leong[a,b,1], Leon C. Ho[a,b], Patrick P. Gao[a,b], Eddie C. Wong[a,b], Celia M. Dong[a,b], Xunda Wang[a,b], Jufang He[c], Ying-Shing Chan[d], Lee Wei Lim[d], and Ed X. Wu[a,b,d,e,2]

[a]Laboratory of Biomedical Imaging and Signal Processing, The University of Hong Kong, Pokfulam, Hong Kong SAR, China; [b]Department of Electrical and Electronic Engineering, The University of Hong Kong, Pokfulam, Hong Kong SAR, China; [c]Department of Biomedical Sciences, City University of Hong Kong, Kowloon, Hong Kong SAR, China; [d]School of Biomedical Sciences, Li Ka Shing Faculty of Medicine, The University of Hong Kong, Pokfulam, Hong Kong SAR, China; and [e]State Key Laboratory of Pharmaceutical Biotechnology, The University of Hong Kong, Pokfulam, Hong Kong SAR, China

Edited by Marcus E. Raichle, Washington University in St. Louis, St. Louis, MO, and approved July 7, 2017 (received for review February 27, 2017)

The hippocampus, including the dorsal dentate gyrus (dDG), and cortex engage in bidirectional communication. We propose that low-frequency activity in hippocampal–cortical pathways contributes to brain-wide resting-state connectivity to integrate sensory information. Using optogenetic stimulation and brain-wide fMRI and resting-state fMRI (rsfMRI), we determined the large-scale effects of spatiotemporal-specific downstream propagation of hippocampal activity. Low-frequency (1 Hz), but not high-frequency (40 Hz), stimulation of dDG excitatory neurons evoked robust cortical and subcortical brain-wide fMRI responses. More importantly, it enhanced interhemispheric rsfMRI connectivity in various cortices and hippocampus. Subsequent local field potential recordings revealed an increase in slow oscillations in dorsal hippocampus and visual cortex, interhemispheric visual cortical connectivity, and hippocampal–cortical connectivity. Meanwhile, pharmacological inactivation of dDG neurons decreased interhemispheric rsfMRI connectivity. Functionally, visually evoked fMRI responses in visual regions also increased during and after low-frequency dDG stimulation. Together, our results indicate that low-frequency activity robustly propagates in the dorsal hippocampal–cortical pathway, drives interhemispheric cortical rsfMRI connectivity, and mediates visual processing.

hippocampus | resting-state functional connectivity | optogenetic | fMRI | low frequency

The hippocampus (HP) plays a prominent role in central nervous system functions, particularly in episodic memory (1, 2) and spatial navigation (3, 4). The HP, including the dentate gyrus (DG), can evoke large-scale influences on cortical activity, because the HP receives convergent information from sensory and limbic cortices before sending reciprocal divergent projections to create a highly interactive corticohippocampal–cortical network. The HP, including DG, CA3, and CA1, and neocortex, are connected via the entorhinal cortex (EC) (5, 6), such that the dorsolateral-to-ventromedial projection that originates in the EC corresponds to a dorsoventral axis of termination in the HP (5). This anatomical topography suggests that a functional gradient could exist along the HP dorsoventral axis. Previous studies demonstrated that dorsal HP (dHP) and cortex are functionally integrated during sensory processing and memory consolidation (7–9). Specifically, dHP can integrate multimodal sensory information and process memory operations (7) using excitatory long-range projections (10). This process occurs over multiple brain circuits, but the role of dHP in complex networks, particularly its influence on brain-wide functional connectivity, is not well understood.

Resting-state functional MRI (rsfMRI) (11–14) provides an invaluable, noninvasive imaging technique to map long-range, brain-wide functional connectivity networks based on the temporal coherence of infraslow (0.005–0.1 Hz) blood oxygen level dependent (BOLD) activity. The functional relevance of specific brain-wide networks in cognition can be inferred through rsfMRI connectivity. Numerous studies demonstrate that changes in rsfMRI connectivity are highly correlated to sensory, memory, and learning task performance, detailed in two comprehensive review papers (13, 15). These studies indicate that changes in brain-wide functional connectivity facilitate and modulate diverse cognitive functions. Despite the enormous potential inherent in this technique, the neural basis of rsfMRI connectivity remains unknown, which impedes further interpretation of neural activity and interactions within and between brain networks. Previous attempts to uncover the neural basis of rsfMRI in anesthetized rats and awake macaques implicated delta oscillations (16, 17) and alpha oscillations (18, 19), respectively. Furthermore, cortical slow oscillations (<1 Hz) (20, 21) resemble the spatiotemporal characteristics of infraslow coherent activity in brain-wide functional networks detected by rsfMRI. Previous studies suggest that these cortical oscillations may underlie rsfMRI connectivity (22–24). Further, a recent study indicates the coupling between resting-state hemodynamics and the oscillatory activity of excitatory neurons (25). However, the answer remains generally inconclusive due to the correlative nature of those studies without directly probing the effects of modulating the brain's electrical activity during rsfMRI.

Brain-wide slow oscillations are a characteristic feature of the mammalian neocortex that occurs spontaneously in the virtual absence of sensory stimulation, such as during anesthesia (26, 27), natural sleep (9, 28), or quiescent waking (29). Previous

Significance

The hippocampus with its dense reciprocal axonal projections to and from cortex is widely believed to mediate numerous cognitive functions. However, it is unknown whether and how specific hippocampal–cortical activity contributes to the brain-wide functional connectivity. Here, we use optogenetics and fMRI to examine how excitatory neural activity initiated in the dorsal dentate gyrus of the hippocampus propagates and modulates resting-state fMRI (rsfMRI) connectivity. We discover its robust propagation brain-wide at low frequency (1 Hz), which enhances interhemispheric rsfMRI connectivity and cortical and subcortical visual responses. Our findings highlight the important role of slow hippocampal–cortical oscillatory activity in driving brain-wide rsfMRI connectivity and mediating sensory processing.

Author contributions: R.W.C., A.T.L.L., and E.X.W. designed research; R.W.C., A.T.L.L., and E.X.W. performed research; R.W.C., A.T.L.L., L.C.H., P.P.G., E.C.W., C.M.D., X.W., J.H., Y.-S.C., L.W.L., and E.X.W. analyzed data; E.C.W., C.M.D., X.W., J.H., and L.W.L. provided technical assistance; and R.W.C., A.T.L.L., and E.X.W. wrote the paper.

The authors declare no conflict of interest.

This article is a PNAS Direct Submission.

Freely available online through the PNAS open access option.

[1]R.W.C. and A.T.L.L. contributed equally to this work.

[2]To whom correspondence should be addressed. Email: ewu@eee.hku.hk.

This article contains supporting information online at www.pnas.org/lookup/suppl/doi:10.1073/pnas.1703309114/-/DCSupplemental.

www.pnas.org/cgi/doi/10.1073/pnas.1703309114

studies also found similar slow oscillatory activities in the hippocampus (30, 31). In particular, DG granule cells modulate hippocampal slow oscillations phase locked to neocortical slow oscillations with a short delay (31). This dynamic property suggests that individual hippocampal neurons can form functional connections with other neurons to create synchronized networks, particularly in slow oscillation frequency ranges, to mediate complex cognitive functions. Such functional coupling may establish the temporal framework for coordinated information transfer within and between networks. Human rsfMRI studies

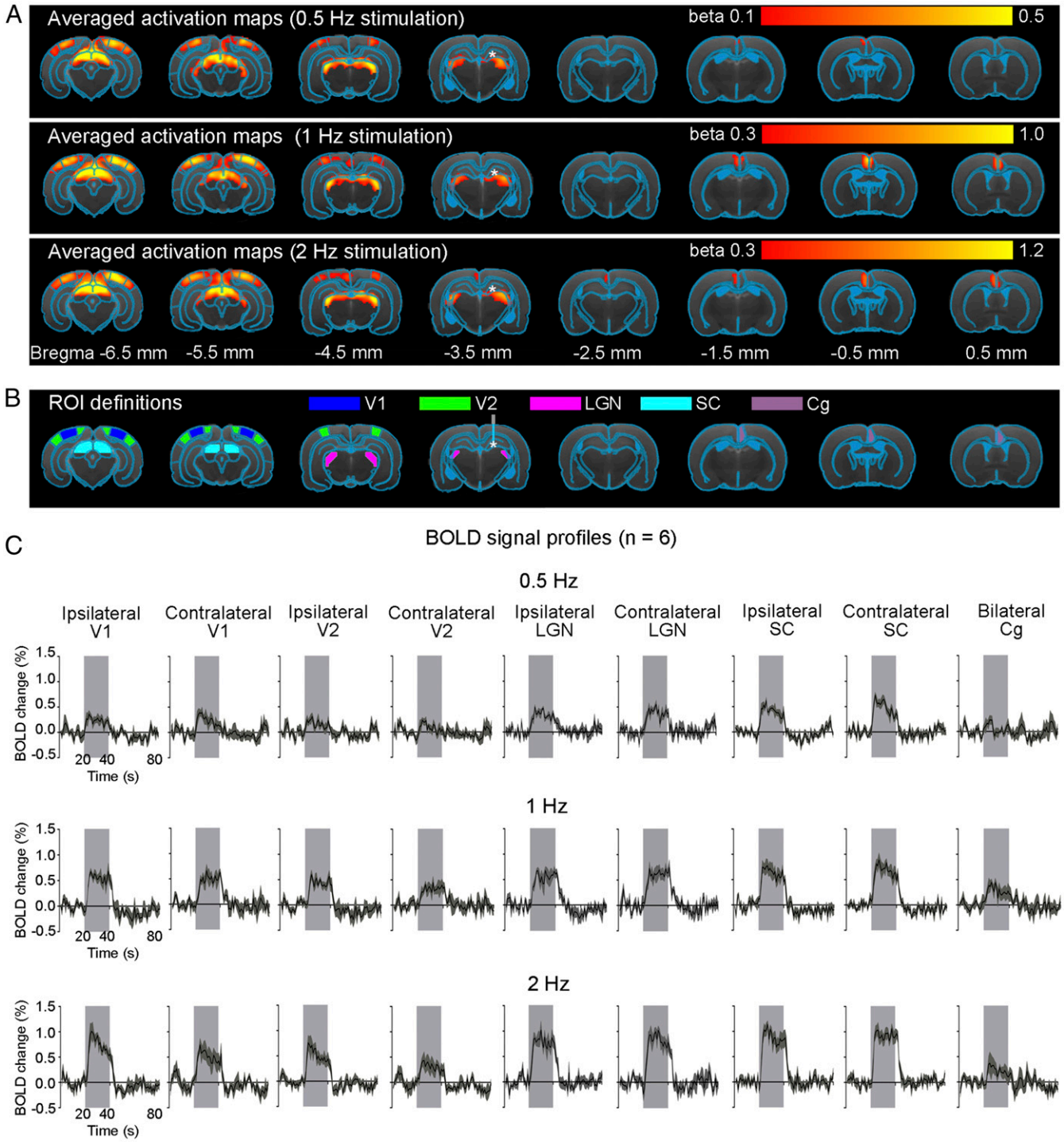

Fig. 1. Brain-wide activation of visually related regions during low-frequency optogenetic stimulation of dDG excitatory neurons in dHP. (*A*) Averaged activation maps at 0.5-Hz (*Top*), 1-Hz (*Middle*), and 2-Hz (*Bottom*) stimulation. * indicates the stimulation site. Robust positive BOLD responses detected in bilateral V1, V2, LGN, and SC, as well as Cg ($n = 6$; $t > 3.1$, corresponding to $P < 0.001$). We used a lower statistical threshold ($t > 2.5$, corresponding to $P < 0.01$) for 0.5-Hz stimulation to detect the low BOLD responses. (*B*) Regions of interest (ROIs) defined by the rat brain atlas to extract the BOLD signal profiles. Abbreviations: g, cingulate cortex; LGN, lateral geniculate nucleus; SC, superior colliculus; V1, primary visual cortex; V2, secondary visual cortex. (*C*) The respective BOLD signal profiles extracted from the ROIs. Error bars indicate ±SEM.

also identified the hippocampus as a densely connected region that may coordinate brain functional connectivity (32–34). Furthermore, a recent study demonstrated the propagation of low-frequency activity from the hippocampus to the cortex in humans (34). Thus, directly examining hippocampal activity with respect to brain-wide propagation and connectivity is essential to uncover the fundamental neural basis of rsfMRI.

Currently, there is no direct evidence that demonstrates the influence of low-frequency activity or oscillations that propagate along the hippocampal–cortical axis on brain-wide rsfMRI connectivity. Because the DG primarily receives cortical terminal projections and acts as a bridge for corticohippocampal–cortical network communication, we examined how spatiotemporally specific activity initiated in the dorsal DG (dDG) influences cortical activity and subsequent brain-wide rsfMRI connectivity by combining optogenetic, cell-specific stimulation of Ca^{2+}/calmodulin-dependent protein kinase IIa (CaMKIIα)-expressing excitatory neurons (i.e., dDG granule cells) and large-scale fMRI detection (35–38). We also examined the functional effects of such changes in brain-wide rsfMRI connectivity on sensory processing.

Results

fMRI Reveals Brain-Wide Frequency-Dependent Activity Propagation from Dorsal Hippocampus. We used virally mediated optogenetics to selectively stimulate CaMKIIα-expressing excitatory neurons in dDG in normal adult male rats. Anatomical MRI scans confirmed the location of the virus injection and optical fiber implantation in dDG of all animals (Fig. S1*A*). Immunohistochemistry confirmed that $CaMKII\alpha^+$ excitatory neurons of the dDG, but not the GABAergic inhibitory neurons, expressed ChR2-mCherry (Fig. S1 *B* and *C*). Whole-brain fMRI determined frequency-dependent spatiotemporal characteristics of brain-wide, long-range evoked responses driven by dDG stimulation using a block design. We performed optogenetic stimulation in lightly anesthetized rats (1% isoflurane). Blue light pulses at four frequencies (0.5 Hz, 1 Hz, 2 Hz, and 40 Hz with 5%, 10%, 20%, and 30% pulse width duty cycle, respectively; light intensity, 40 mW/mm^2) were delivered to dDG neurons in a block design paradigm. We chose reduced duty cycles for 0.5-Hz, l-Hz, and 2-Hz stimulation to avoid excessively long stimulation pulse widths that may not be physiological.

A 1-Hz optogenetic stimulation of dDG evoked positive and robust BOLD responses in bilateral primary visual cortex (V1), secondary visual cortex (V2), lateral geniculate nucleus (LGN) and superior colliculus (SC), as well as the cingulate cortex (Cg) (Fig. 1 *A* and *C*). We observed similar BOLD responses at 0.5- and 2-Hz stimulations (Fig. 1 *A* and *C*). We also stimulated dDG at a higher frequency (40 Hz) and observed strong positive responses in bilateral dHP and negative responses in bilateral ventral HP (vHP) and Cg (Fig. 2 *A* and *C*). However, we detected no responses in V1, V2, LGN, and SC (Fig. S2). The sequence of fMRI responsivity demonstrates spatiotemporal response properties from dHP shifting from regions actively involved in processing visual information and cognition at low frequencies (0.5–2 Hz) to local hippocampal regions (40 Hz). The absolute BOLD signal amplitude in bilateral V1 at 0.5 Hz was generally lower than those at 1 Hz and 2 Hz, mainly due to the reduced pulse width duty cycle of 5% used at 0.5 Hz.

To gain insight into the fMRI findings, we performed extracellular electrophysiological recordings using low-impedance (1 MΩ) electrodes to characterize downstream signal propagation from dDG excitatory neurons in dHP to V1 using identical stimulation paradigms (Fig. 3*A*). Local field potentials (LFPs), which are highly correlated with BOLD signals (39), revealed that only low-frequency stimulation (0.5–2 Hz) evoked strong LFP responses in bilateral V1 (Fig. 3*B*), corroborating the fMRI results (Fig. 1), although all tested stimulation frequencies evoked LFP responses in dDG/dHP. We further investigated the response latencies to determine the dynamic properties within the hippocampal–cortical circuit. Following dDG stimulation, evoked responses first occurred in the ipsilateral dHP, followed

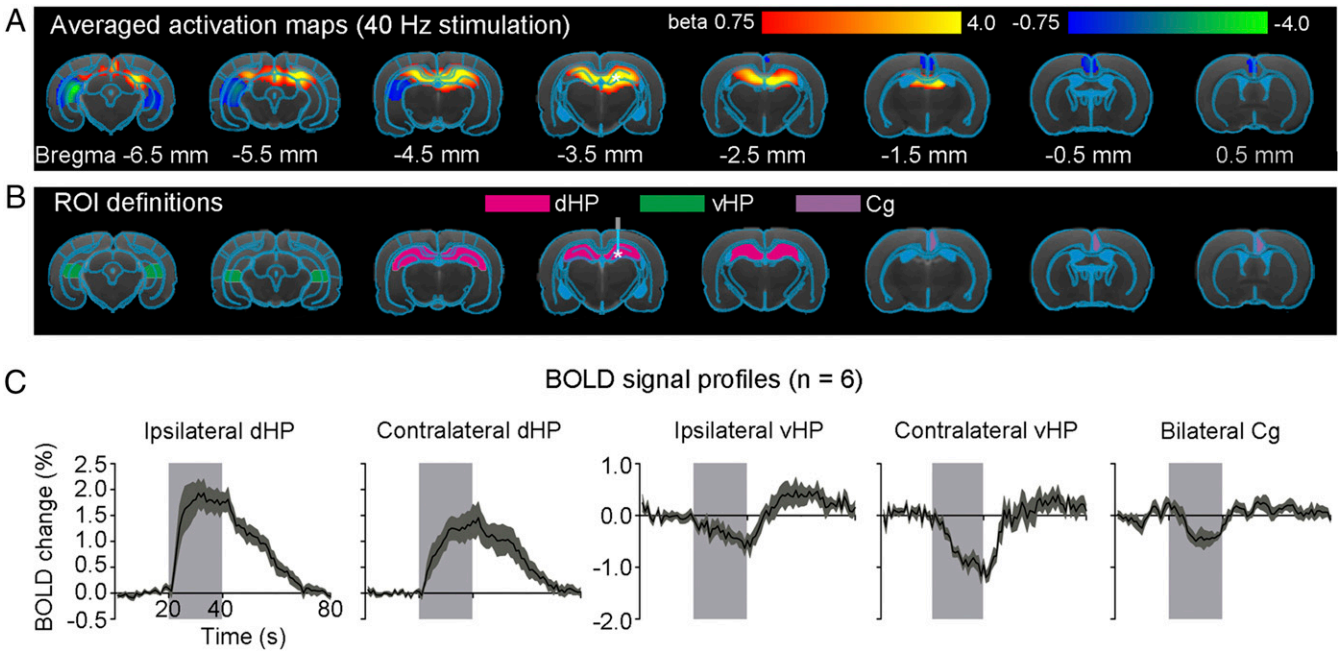

Fig. 2. Local hippocampal activation and deactivation during 40-Hz optogenetic stimulation of dDG excitatory neurons in dHP. (*A*) Averaged activation maps at 40-Hz stimulation. * indicates the stimulation site. Robust positive BOLD responses are detected in bilateral dHP, whereas negative responses are detected in the bilateral vHP and Cg ($n = 6$; $t > 3.1$ or $t < -3.1$, corresponding to $P < 0.001$). (*B*) Regions of interest (ROIs) are based on the rat brain atlas to extract bold signal profiles. Abbreviations: Cg, cingulate cortex; dHP, dorsal hippocampus; vHP, ventral hippocampus. (*C*) BOLD signal profiles extracted from the ROIs. Error bars indicate ±SEM.

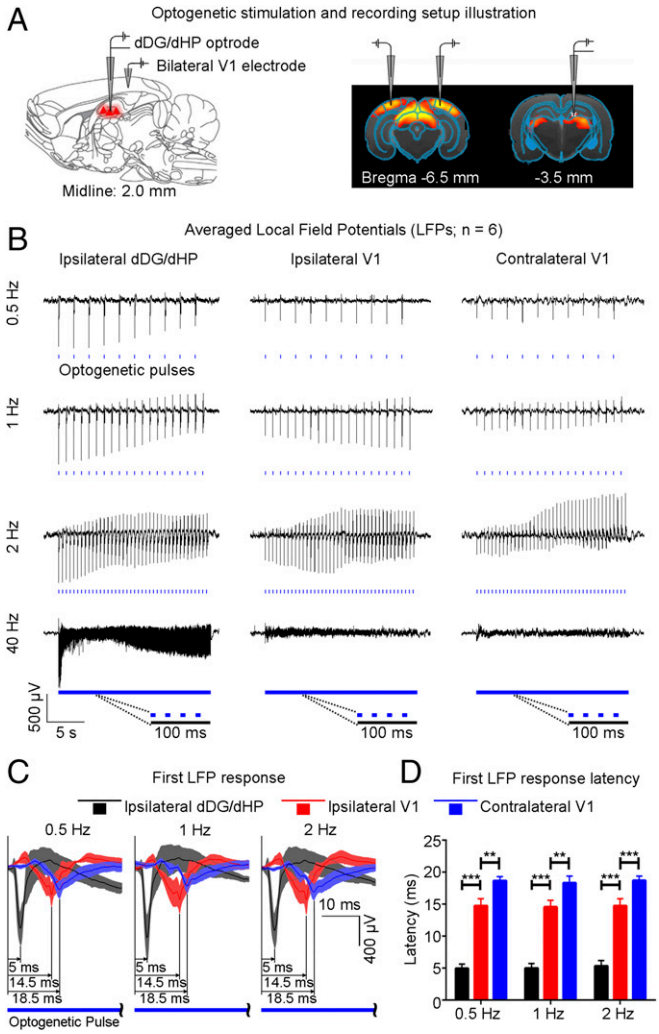

Fig. 3. Local field potentials (LFPs) in ipsilateral dDG/dHP and bilateral V1 confirm neuronal activity underlies BOLD fMRI responses, and latency measurements indicate polysynaptic propagation of low-frequency activity from dHP. (*A*) Recording electrodes location in ipsilateral dDG/dHP and bilateral V1. (*B*) Averaged LFP traces in ipsilateral dDG/dHP and bilateral V1 for 0.5-Hz, 1-Hz, 2-Hz, and 40-Hz stimulation ($n = 6$). All frequencies evoked responses in ipsilateral dDG/dHP. Only low-frequency stimulation evoked strong responses in bilateral V1. (*C*) LFP responses from the first optogenetic pulse for 0.5-Hz, 1-Hz, and 2-Hz stimulation. Error bars indicate ±SEM. (*D*) Latency measurements of the first LFP response during low-frequency stimulation (0.5 Hz: ipsilateral dDG/dHP = 4.95 ± 0.71 ms, ipsilateral V1 = 14.77 ± 1.08 ms, contralateral V1 = 18.68 ± 0.65 ms; 1 Hz: ipsilateral dDG/dHP = 5.02 ± 0.71 ms, ipsilateral V1 = 14.57 ± 1.03 ms, contralateral V1 = 18.33 ± 1.06 ms; 2 Hz: ipsilateral dDG/dHP = 5.35 ± 0.85 ms, ipsilateral V1 = 14.77 ± 1.09 ms, contralateral V1 = 18.72 ± 0.68 ms; one-way ANOVA followed by Bonferroni's post hoc test; $^{**}P < 0.01$ and $^{***}P < 0.001$). Error bars indicate ±SEM.

by the ipsilateral V1, and finally the contralateral V1 (Fig. 3*C*). Latency was measured at the first prominent trough of the optogenetically evoked LFP response. Latency measurements were similar for 0.5-Hz, 1-Hz, and 2-Hz stimulation (0.5 Hz: ipsilateral dDG/dHP = 4.95 ± 0.71 ms, ipsilateral V1 = 14.77 ± 1.08 ms, contralateral V1 = 18.68 ± 0.65 ms; 1 Hz: ipsilateral dDG/dHP = 5.02 ± 0.71 ms, ipsilateral V1 = 14.57 ± 1.03 ms, contralateral V1 = 18.33 ± 1.06 ms; and 2 Hz: ipsilateral dDG/dHP = 5.35 ± 0.85 ms, ipsilateral V1 = 14.77 ± 1.09 ms, contralateral V1 = 18.72 ± 0.68 ms) (Fig. 3*D*). Although optogenetically evoked LFP profiles evolved throughout the stimulation period, the comparative latency measurements between the first and last response were similar (Fig. S3), demonstrating stable response latencies. These latency measurements indicate that the first evoked responses occurred in the ipsilateral dDG/dHP and propagated to the ipsilateral V1 polysynaptically (9.5 ± 1.3 ms, $P < 0.001$; one-way ANOVA followed by Bonferroni's post hoc test), before reaching contralateral V1 via monosynaptic interhemispheric callosal connections (40) (4.0 ± 1.5 ms, $P < 0.01$; one-way ANOVA followed by Bonferroni's post hoc test). However, we do not preclude that propagation to contralateral V1 can occur polysynaptically through contralateral dHP. No evoked responses were observed in the naïve animal (Fig. S4), indicating that the observed responses were a direct result of ChR2 stimulation, not photoelectrically induced artifacts or undesired light-induced activations of the visual pathway. In addition, multiunit activity (MUA) recordings in dDG showed all stimulation frequencies successfully elicited hippocampal spikes without failure (Fig. S5). We made the exposed optical fiber cannula (used to deliver blue light pulses) opaque using heat shrinkable sleeves in all MRI and electrophysiological recording experiments to prevent light leakage that may cause undesired visual stimulation to animals.

Low-Frequency Optogenetic Stimulation of dDG Excitatory Neurons in dHP Enhances Brain-Wide Resting-State Functional Connectivity. Next, we examined the effects of low-frequency activity propagating along the dorsal hippocampal–cortical pathway (Figs. 1 and 3) on interhemispheric or bilateral rsfMRI connectivity (Fig. 4*A*). Before the rsfMRI acquisition, we measured LFPs in dDG/dHP and V1 to ensure that sustained 1-Hz stimulation (400 s) did not evoke different LFP response characteristics observed during shorter stimulation durations (20 s) (Fig. S6 vs. Fig. 3*B*). LFPs showed steady evoked responses, which demonstrate the stability of 1-Hz evoked responses in both stimulated and activated regions. The strength of interhemispheric rsfMRI connectivity increased progressively in dHP, V1, primary auditory cortex (A1), and primary somatosensory cortex (S1) during (during) and after (post) 1-Hz dDG stimulation, which showed an increase in the spatial extent of connectivity maps (Fig. 4*B*, *Left*). The interhemispheric rsfMRI connectivity strengthened significantly during stimulation in dHP, V1, A1, and S1 (Fig. 4*B*, *Middle*; $n = 18$; dHP: 37.3 ± 7.4%, $P < 0.01$; V1: 55.6 ± 11.5%, $P < 0.01$; A1: 44.2 ± 6.9%, $P < 0.05$; and S1: 43.3 ± 9.0%, $P < 0.01$; one-way ANOVA followed by Bonferroni's post hoc test). We also observed a significant enhancement of interhemispheric rsfMRI connectivity post stimulation (Fig. 4*B*, *Middle*; $n = 18$; dHP: 46.2 ± 8.6%, $P < 0.001$; V1: 72.9 ± 13.8%, $P < 0.001$; A1: 53.9 ± 7.6%, $P < 0.01$; and S1: 58.9 ± 10.9%, $P < 0.001$; one-way ANOVA followed by Bonferroni's post hoc test). We then computed the connectivity spectrum of rsfMRI signals that were bilaterally correlated. We observed an increase in infraslow (<0.1 Hz) rsfMRI BOLD activity in dHP, V1, A1, and S1 during and post stimulation (Fig. 4*B*, *Right*). We further examined the intrahemispheric or local rsfMRI connectivity, which was increased during (Fig. 4*C*, *Left*; $n = 18$; ipsilateral dHP: 59.6 ± 8.6%, $P < 0.001$; contralateral dHP: 55.6 ± 8.2%, $P < 0.01$; ipsilateral S1: 38.3 ± 9.4%, $P < 0.05$; and contralateral S1: 45.6 ± 8.7%, $P < 0.01$; one-way ANOVA followed by Bonferroni's post hoc test) and post stimulation (Fig. 4*C*; $n = 18$; ipsilateral dHP: 58.4 ± 6.9%, $P < 0.01$; contralateral dHP: 57.4 ± 6.8%, $P < 0.01$; ipsilateral V1: 43.8 ± 5.4%, $P < 0.01$; contralateral V1: 45.7 ± 11.3%, $P < 0.01$; contralateral A1: 33.7 ± 7.3%, $P < 0.05$; ipsilateral S1: 51.2 ± 7.7%, $P < 0.01$; and contralateral S1: 60.5 ± 13.0%, $P < 0.01$; one-way ANOVA followed by Bonferroni's post hoc test).

We then performed LFP recordings in bilateral V1 and ipsilateral dDG/dHP to determine the neuronal activity underlying enhanced V1 interhemispheric rsfMRI connectivity and examine

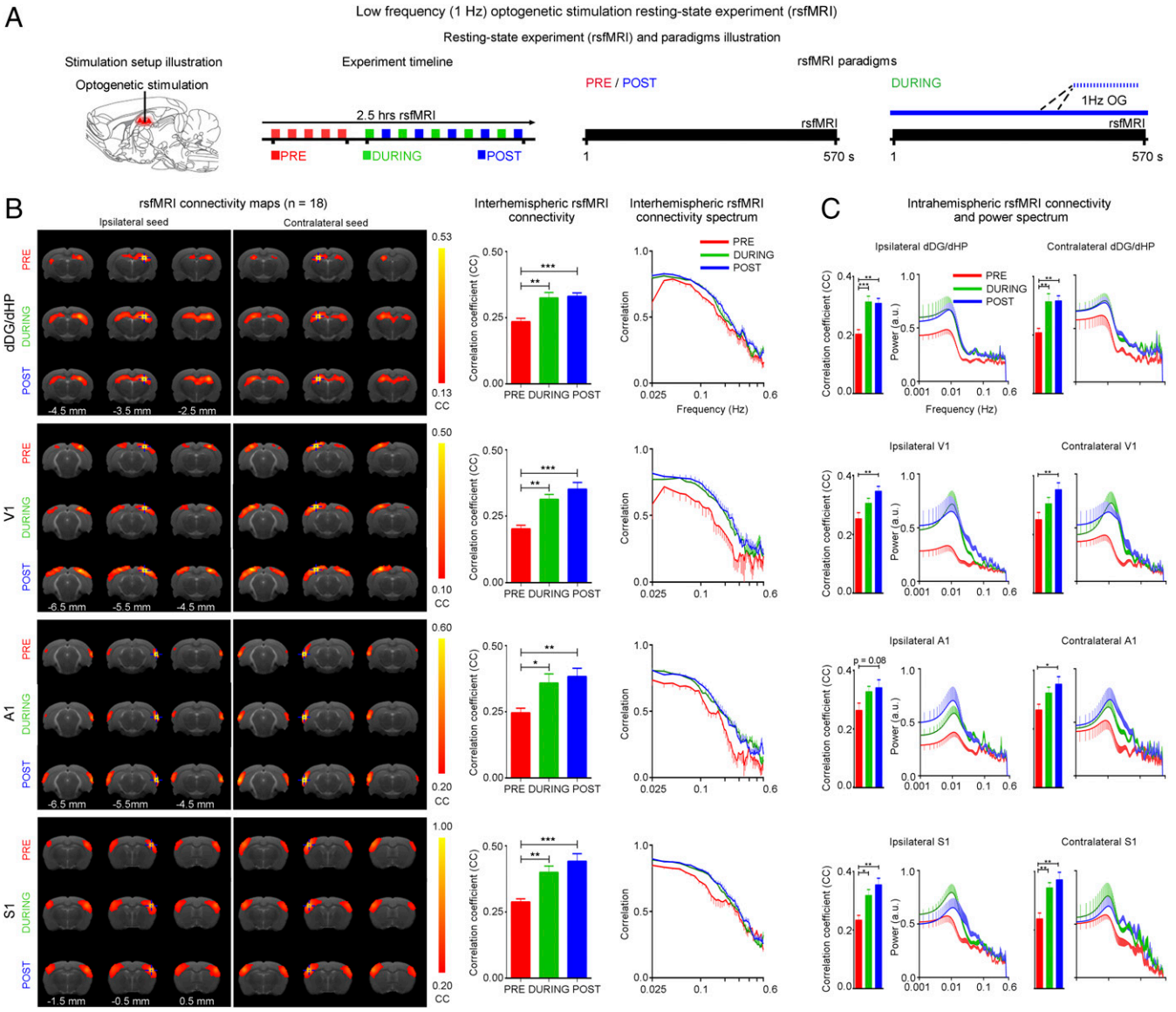

Fig. 4. Increased interhemispheric rsfMRI connectivity during (during) and after (post) low-frequency (1 Hz) optogenetic stimulation of dDG excitatory neurons in dHP. (*A*) Schematic of the optogenetic stimulation setup (*Left*), a typical rsfMRI experiment timeline with five baseline (pre) scans acquired before five "during" scans interleaved with five post scans (*Middle*), and the corresponding rsfMRI paradigms used (*Right*). (*B*) RsfMRI connectivity maps of dHP, V1, A1, and S1 (*Left*), corresponding quantification of interhemispheric connectivity (*Middle*), and their respective connectivity spectrum (*Right*), pre, during, and post low-frequency optogenetic stimulation. rsfMRI maps generated by correlation analysis of band-pass filtered (0.005–0.1 Hz) BOLD signals using a seed defined in the ipsilateral and contralateral side. Seed location is indicated by a blue crosshair. Quantification of the interhemispheric rsfMRI connectivity (n = 18; one-way ANOVA followed by Bonferroni's post hoc test; $*P < 0.05$, $**P < 0.01$, and $***P < 0.001$; error bars indicate ±SEM). (*C*) Quantification of intrahemispheric rsfMRI connectivity (*Left*) and the respective power spectrum (*Right*) of ipsilateral and contralateral dHP, V1, A1, and S1.

possible interregional (i.e., dDG/dHP–V1) connectivity changes after low-frequency optogenetic stimulation under similar conditions to rsfMRI experiments (Fig. 5*A*). We computed the ipsilateral dDG/dHP and bilateral V1 intrahemispheric LFP frequency spectra (Fig. 5*B*), as well as the V1–V1 interhemispheric and dDG/dHP–V1 LFP interregional connectivity spectra (Fig. 5*C*). We observed a pronounced peak at ∼1 Hz in ipsilateral dDG/dHP and bilateral V1 intrahemispheric LFP spectrum during and post stimulation (Fig. 5*A*) and found a general increase of slow (0.1–1 Hz) and delta (1–4 Hz) oscillations (Fig. 5*A*), indicating a persistent modulation of LFP activity by low-frequency optogenetic stimulation of dDG excitatory neurons. The connectivity spectra demonstrate that the bilateral V1, ipsilateral dDG/dHP–ipsilateral V1, and ipsilateral dDG/dHP–contralateral V1 correlation of slow and delta oscillations strengthened during and post stimulation (Fig. 5*C*). These results indicate that persistent low-frequency activity propagating from dDG/dHP along the hippocampal–cortical pathway enhances interhemispheric rsfMRI connectivity. They demonstrate that increased slow and delta oscillations, in addition to the increased infraslow rsfMRI BOLD activity, contribute to enhanced brain-wide rsfMRI connectivity. These results further suggest significant effects on the integration of sensory information and memory operations, because such functions normally occur via cross-frequency coupling mechanisms between co-occurring brain oscillations (41).

High-Frequency Stimulation of dDG Excitatory Neurons in dHP Does Not Enhance Brain-Wide Resting-State fMRI Connectivity. Separate rsfMRI experiments (n = 8) examined high-frequency stimulation (40 Hz) (Fig. 6*A*). No significant increase in inter- and

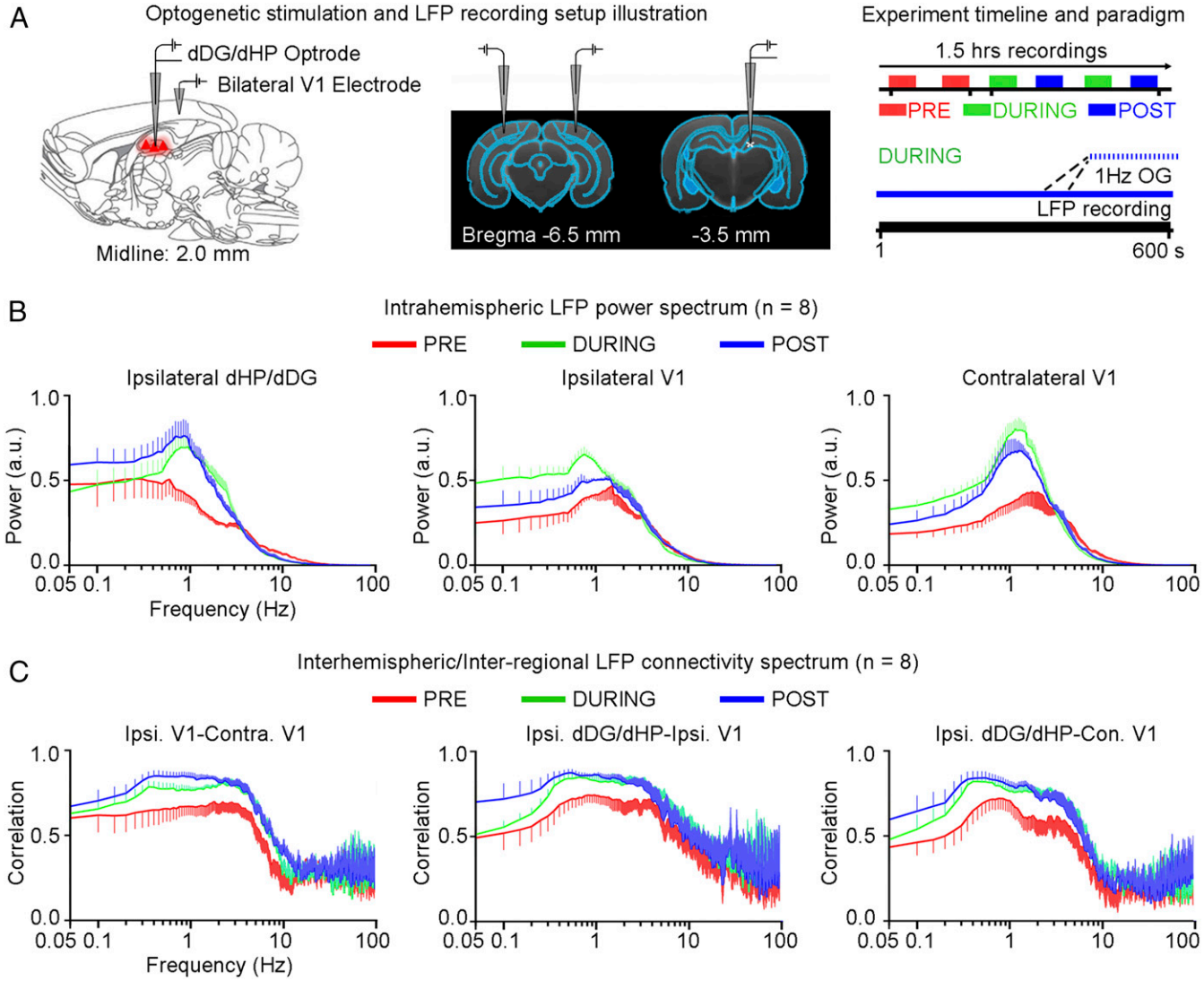

Fig. 5. Increased slow (0.1–1 Hz) and delta (1–4 Hz) neuronal oscillations during (during) and after (post) low-frequency (1 Hz) optogenetic stimulation of dDG excitatory neurons in dHP. (*A*) Illustration of LFP recording electrode location in ipsilateral dDG/dHP and bilateral V1 (*Left*) and a typical LFP recording experiment timeline with the corresponding paradigms (*Right*). (*B*) Intrahemispheric LFP power spectrum of ipsilateral dDG/dHP and bilateral V1. Error bars indicate ±SEM. (*C*) LFP connectivity spectra for interhemispheric V1–V1 and interregional dDG/dHP–V1. Error bars indicate ±SEM.

intrahemispheric rsfMRI connectivity was observed during (during) and after (post) 40 Hz optogenetic stimulation of dDG (Fig. 6). Only interhemispheric rsfMRI connectivity in dHP exhibited a significant decrease in strength. These results demonstrate that only low-frequency activity enhances brain-wide functional connectivity.

Pharmacologically Blocking dDG Neurons in dHP Decreases Brain-Wide Resting-State fMRI Connectivity. We examined the effects of pharmacologically inactivating dDG neurons in dHP on rsfMRI interhemispheric connectivity using tetrodotoxin (TTX). rsfMRI was acquired before (pre) and after (post) infusion of TTX (Fig. 7*A*). Pharmacological blockade significantly decreased rsfMRI interhemispheric connectivity in dHP, V1, A1, and S1, and intrahemispheric connectivity in dHP and V1 (Fig. 7 *B* and *C*). These results present additional evidence that dHP is a pivotal structure that coordinates brain-wide rsfMRI connectivity.

Low-Frequency Stimulation of dDG Excitatory Neurons in dHP Enhances Visually Evoked fMRI Responses. To investigate functional effects of low-frequency dorsal hippocampal–cortical activity on visual processing, visual fMRI (vfMRI) was performed before (pre), during (during), and after (post) continuous 1-Hz optogenetic stimulation (Fig. 8*A*). Visually evoked BOLD responses occurred along the visual pathway, including bilateral LGN, SC, and VC (Fig. 8 *B* and *C*). However, BOLD responses increased in ipsilateral LGN and bilateral SC during stimulation (Fig. 8*D*) (n = 8; ipsilateral LGN: 37.9 ± 19.8%, $P < 0.05$; ipsilateral SC: 49.2 ± 28.1%, $P < 0.05$; contralateral SC: 38.6 ± 14.5%, $P < 0.05$; one-way ANOVA followed by Bonferroni's post hoc test). BOLD responses further increased in bilateral VC, LGN and SC post stimulation (Fig. 8*D*) (n = 8; ipsilateral VC: 93.4 ± 28.9%, $P < 0.01$; contralateral VC: 87.2 ± 14.2%, $P < 0.01$; ipsilateral LGN: 80.9 ± 18.5%, $P < 0.01$; contralateral LGN: 71.0 ± 25.3%, $P < 0.01$; ipsilateral SC: 136.5 ± 40.1%, $P < 0.01$; contralateral SC: 105.9 ± 22.0%, $P < 0.01$; one-way ANOVA followed by Bonferroni's post hoc test). These results indicate that persistent low-frequency activity propagating along hippocampal–cortical pathways can enhance sensory responses that underlie sensory processing.

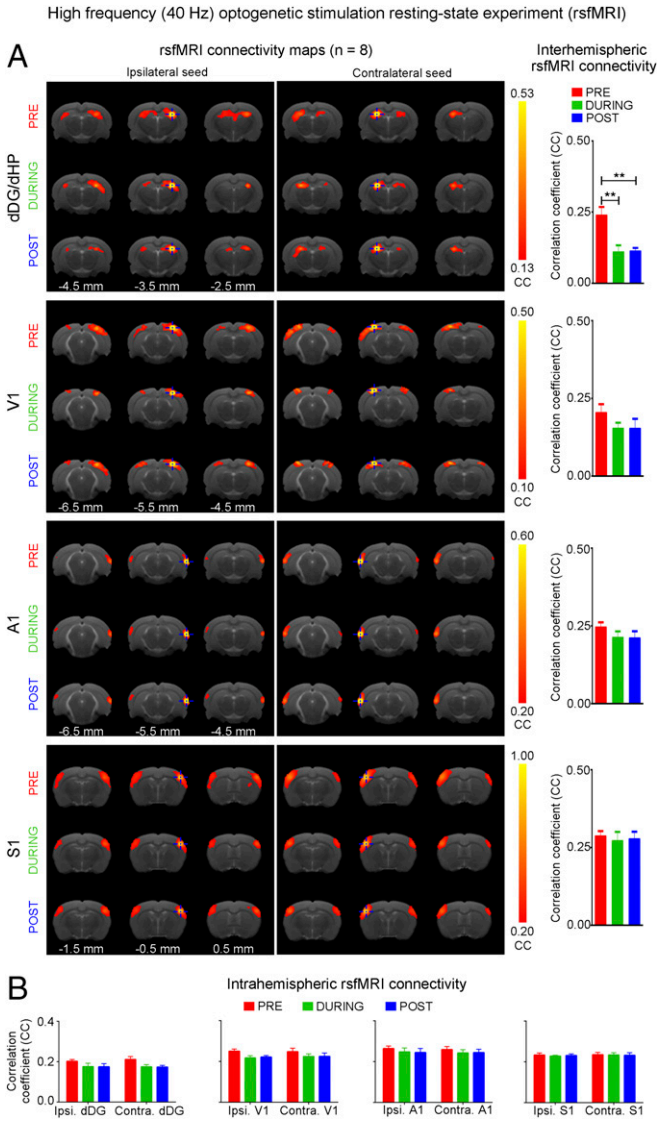

Fig. 6. High-frequency (40 Hz) optogenetic stimulation of dDG excitatory neurons in dHP does not enhance interhemispheric rsfMRI connectivity. (*A*) rsfMRI connectivity maps of dHP, V1, A1, and S1 before (pre), during (during), and after (post) high-frequency optogenetic stimulation (*Left*) and the corresponding quantification of interhemispheric rsfMRI connectivity (*Right*). (*B*) Quantification of intrahemispheric rsfMRI connectivity.

Discussion

Here, we examined large-scale effects of spatiotemporal-specific propagation of downstream hippocampal activity using optogenetic stimulation and brain-wide fMRI and rsfMRI. Stimulation of dDG excitatory neurons at low frequency, but not high frequency, evoked robust cortical and subcortical brain-wide responses. This low-frequency stimulation enhanced interhemispheric hippocampal and cortical rsfMRI connectivity. LFP recordings revealed an increase in slow oscillations in dHP and visual cortex (VC), interhemispheric visual cortical connectivity, and hippocampal–cortical connectivity. Meanwhile, pharmacological inactivation of dorsal hippocampus decreased brain-wide rsfMRI connectivity. Functionally, visually evoked fMRI responses in visual regions also increased during and after low-frequency dHP stimulation. Together, these experimental results highlight the role of low-frequency activity propagating along the hippocampal–cortical pathway, particularly its contribution to interhemispheric cortical rsfMRI connectivity.

Our fMRI results and electrophysiological recordings demonstrate that the anatomical topography within HP is spatiotemporally specific with low-frequency activity propagating from dDG/dHP downstream to VC and Cg. Note that a recent human rsfMRI study of low-frequency hippocampal–cortical propagation also showed characteristics of activity propagation between the hippocampus and visual cortex (34). Interestingly, the robust detection of BOLD responses in bilateral visual cortices observed in the present study suggests that low-frequency activity initiated in dDG may drive slow oscillatory activity to coordinate visual memory replay in the visual cortex and hippocampus

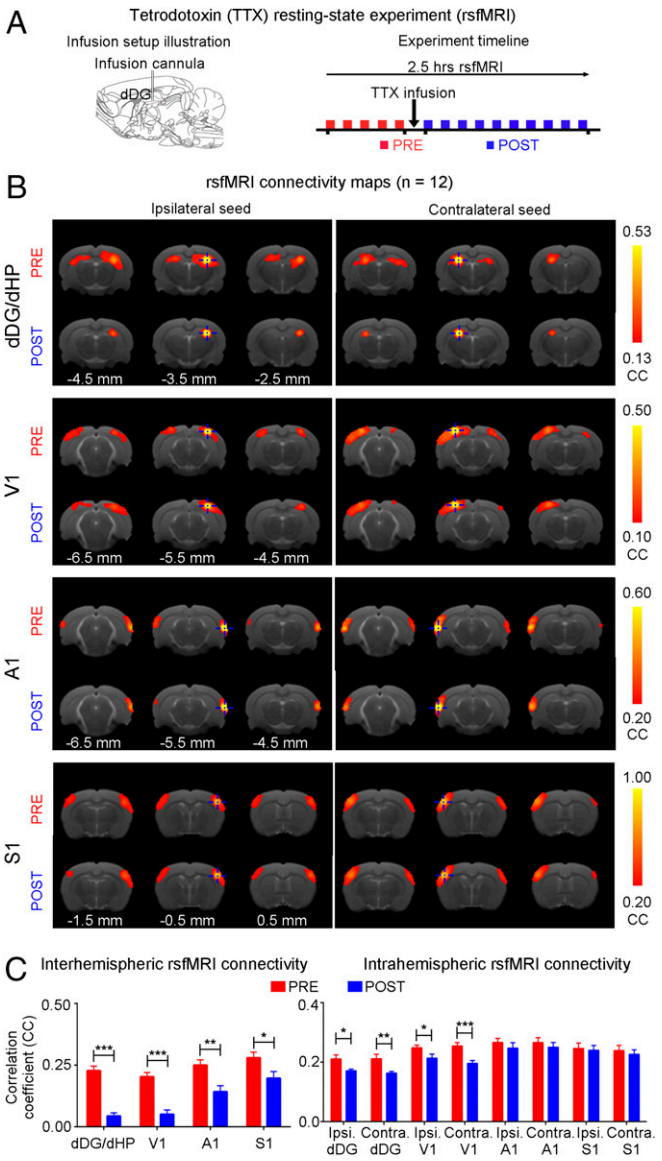

Fig. 7. Pharmacological inactivation of dDG neurons in dHP decreases interhemispheric rsfMRI connectivity. (*A*) Illustration of the tetrodotoxin (TTX) infusion setup (*Left*) and a typical rsfMRI experiment timeline whereby TTX is infused into dHP a minute after the last baseline (pre) scan (*Right*). The first post scan is acquired a minute after the completion of TTX infusion. (*B*) rsfMRI connectivity maps of dHP, V1, A1, and S1, pre and post infusion of TTX. (*C*) Quantification of the interhemispheric rsfMRI connectivity (*Left*; $n = 12$; paired t test followed by Bonferroni's post hoc test; $^{*}P < 0.05$, $^{**}P < 0.01$, and $^{***}P < 0.001$; error bars indicate ±SEM).

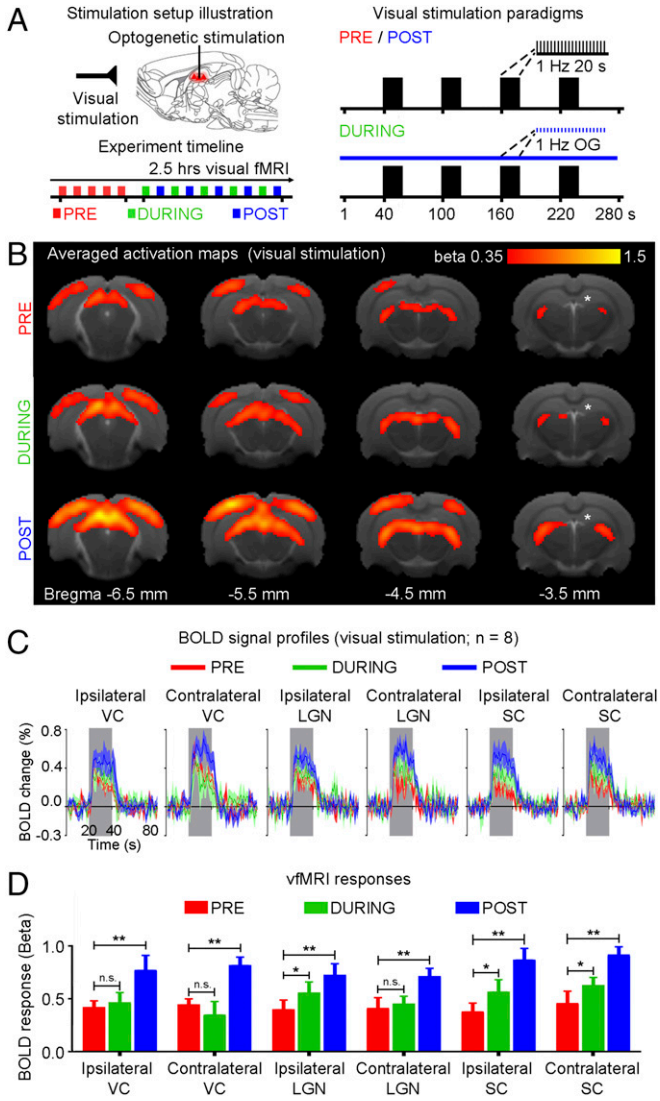

Fig. 8. Low-frequency (1 Hz) optogenetic stimulation of dDG excitatory neurons in dHP enhances visually evoked fMRI responses. (*A*) Illustration of binocular visual and optogenetic fMRI stimulation setup (*Top Left*). Block design visual stimulation paradigm (20 s on, 60 s off) presented before (pre), during (during), and after (post) continuous low-frequency optogenetic stimulation (*Right*). Typically, five baseline visual fMRI scans were acquired before five "during" scans were interleaved with five post scans (*Bottom Left*). (*B*) Averaged activation maps for visual stimulation pre, during, and post low-frequency stimulation. BOLD responses are detected in bilateral V1, V2, LGN, and SC ($n = 8$; $t > 3.1$, corresponding to $P < 0.001$). (*C*) BOLD signal profiles in the bilateral V1, LGN, and SC. Error bars indicate ±SEM. (*D*) Comparison of vfMRI responses (one-way ANOVA followed by Bonferroni's post hoc test; $*P < 0.05$ and $**P < 0.01$; error bars indicate ±SEM).

during slow-wave sleep (9). Although LFP recordings in bilateral V1 only showed robust primary optogenetically evoked responses, we do not preclude that the presence of secondary responses like slow oscillations may contribute to BOLD responses. Moreover, Cg, a prefrontal cortical region implicated in memory (42) and learning (43), was also activated in our fMRI experiments. This result reinforces the role of dHP in cognitive functions.

We do not suggest that the presence of high-frequency activity could not be evoked by our low-frequency optogenetic stimulation. Previous studies showed features of diffuse brain-wide activity that were identified in relation to high-frequency hippocampal sharp wave ripple events (44–46). The relationship between slow oscillations and ripples in the hippocampus and/or cortex is well documented (30, 47–50). In particular, electrophysiological studies demonstrated that a large proportion of endogenous slow oscillations in the cortex and hippocampus precede the generation of hippocampal ripples (47–49). This finding indicates that slow oscillations and ripples are tightly coupled within the hippocampal–cortical pathways.

Low-frequency activity is a key contributor to integrate long-range interactions within thalamocortical–thalamic networks (21, 51–53). A recent study investigated the relationship between single neuron spiking activity and brain-wide cortical calcium dynamics (54). The authors found that thalamic spikes could produce various large-scale cortical activity patterns, which were underpinned by large-scale slow calcium activity (<1 Hz). Complementarily, earlier work using voltage-sensitive dye imaging also showed similar large-scale slow spontaneous cortical activity patterns (55). In fact, our recent study demonstrated brain-wide cortical activity propagation when the somatosensory thalamus was optogenetically stimulated at low frequency (36). Therefore, subcortical regions, such as thalamus, could initiate brain-wide cortical activity.

Our fMRI results and LFP latency analyses suggest that low-frequency activity propagates downstream from ipsilateral dDG/dHP to ipsilateral VC via the ipsilateral lateral EC (LEC) (5), before reaching contralateral VC through the corpus callosum (40, 56) to finally terminate in the LGN and SC via cortico-thalamic and corticocollicular descending projections. The medial EC (MEC) may not actively participate in our observed responses because dHP is functionally coupled with LEC, not MEC, to establish functional gradients along the dorsoventral hippocampal axis (8). In addition, our optogenetic stimulation of dDG reveals unique spatiotemporal response characteristics compared with fMRI studies using CA3 electrical stimulation (57) or optogenetic CA1 stimulation (58). We postulate that different stimulation locations elicit distinct spatiotemporal responses within hippocampal subfields. The hippocampal network encompasses multiple CaMKIIα-excitatory neurons, such as granule cells in DG and pyramidal cells in CA3/CA1, reciprocally connected to a network of GABAergic interneurons (5). Whereas we exclusively stimulated dDG excitatory neurons, orthodromic activation of various intrahippocampal circuits, and subsequent, monosynaptic excitation of interneurons and polysynaptic excitation of CA3/CA1 excitatory cells may occur. Based on our results, we propose that dHP has a frequency-dependent spatiotemporal gradient across hippocampal subfields, such that dDG facilitates downstream propagation of low-frequency activity brain-wide.

Importantly, our study demonstrates that interhemispheric cortical rsfMRI connectivity increases after low-frequency dDG stimulation (Fig. 4). This low-frequency activity propagates downstream from dDG/dHP and underlies changes in neuronal synchrony or neuronal excitability to substantially enhance brain-wide functional connectivity. Indeed, our LFP measurements show that hippocampal–cortical slow and delta oscillations enhance neuronal synchrony in bilateral V1 (Fig. 5). The parallel increase in both interhemispheric rsfMRI connectivity (at infra-slow frequency 0.005–0.1 Hz) and slow- and delta-frequency neuronal oscillations (0.1–4 Hz) indicates a tight association between the two measures, because slow oscillations generate large, synchronous membrane-potential fluctuations in many neurons throughout brain-wide networks (21, 22, 59). Our results demonstrate the modulatory effects of increased neuronal slow oscillations on corticocortical and hippocampal–cortical connectivity. Numerous studies have demonstrated the importance of hippocampal and cortical theta oscillations (4–12 Hz) (60) to coordinate groups of neurons to integrate sensory information (61) and consolidate memory (62, 63). Comparatively, our results suggest that the hippocampus plays an even greater role in coordinating brain-wide neural activity, particularly at slow oscillations.

Whereas we observed increased hippocampal delta oscillations, hippocampal delta activities have been observed so far only in primates and humans but not rodents (64, 65). Previous studies in rodents showed that theta-like oscillations in the hippocampus shifted to lower frequencies (i.e., delta range) during light anesthesia (~1.0% isoflurane) (66, 67). This finding suggests that our increased delta oscillation results might arise from increased theta-like oscillations after low-frequency stimulation.

Whereas we exclusively focused on the dHP in this study, we do not preclude that the vHP could also affect rsfMRI connectivity. Given the differences in anatomical and functional organization (7, 8), the vHP may predominantly affect nonsensory-related regions through unknown mechanisms. Interhemispheric or homotopic rsfMRI connectivity networks are conserved across species (17, 68–70) and under distinct brain states (e.g., anesthesia, sleep, and wake) (71, 72) and consistent among different human subjects (73). We (14, 36) and others (16, 17, 68) have reliably measured interhemispheric rsfMRI connectivity in sensory cortices of rodents under light isoflurane (~1.0%). However, the detection of more complex rsfMRI networks, such as default mode network, could be altered by anesthesia (74).

Brain-wide slow oscillations exhibit two distinct states, namely, up states with vigorous synaptic activity and down states of relative quiescence, that cycle between each other (26, 29). Up states, in particular, can increase neuronal sensitivity to synaptic inputs and enhance their responsiveness to weak, subthreshold inputs (75, 76). Our observed increase in neuronal synchrony of slow oscillatory activity, triggered by low-frequency stimulation of dDG, could modulate incoming signals, such as visual inputs, to promote robust evoked responses and significantly increase interhemispheric rsfMRI connectivity in V1. Studies investigating the dependence of evoked cortical responses on spontaneous network activity in up states demonstrated a linear relationship between spontaneous membrane potential levels and the magnitude of evoked responses in cortical neurons. Such a linear relationship between up-state membrane potential and evoked responses was described in anesthetized cat visual cortex (77, 78). However, our study indicates that this modulation extends beyond cortical regions, because responses to visual inputs increased not only in visual cortices but also in visual subcortical regions.

Hippocampal–cortical activity is state dependent, so the light anesthesia used here may alter their characteristics (34, 66, 67, 79). Nevertheless, prior work revealed synchronized interhemispheric delta oscillations as a major contributor to infraslow rsfMRI connectivity in anesthetized rodents (16, 17). A recent human rsfMRI study demonstrated that low-frequency oscillations, such as delta, propagate from the hippocampus toward cortex and slowly in the opposite direction during sleep (34). An EEG study in humans reported EEG differences under anesthesia and sleep/wake conditions, but the authors observed sleep oscillations (i.e., slow and delta dominant) under anesthesia (80). Such oscillations were also found in rodent studies during extracellular and/or intracellular recordings (67, 81, 82). Taken together, these studies highlight the robust presence of low-frequency activity in brain-wide interactions under various states, including anesthetized and sleep conditions.

In conclusion, our results demonstrate that slow oscillatory activity propagating along dorsal hippocampal–cortical pathways, contributes to interhemispheric cortical connectivity and mediates sensory functions. This finding advances our fundamental understanding of the neural basis and functional role of brain-wide rsfMRI connectivity. Further, we present an integrated optogenetic fMRI approach to interrogate rsfMRI mechanisms and to explore neuromodulation of brain connectivity.

Methods

Subjects. Adult male Sprague Dawley rats (250–300 g) were used in all experiments. Animals were individually housed under a 12-h light/dark cycle with access to food and water ad libitum. All animal experiments were approved by the University of Hong Kong's Committee on the Use of Live Animals in Teaching and Research (CULATR). Group I underwent optogenetic fMRI experiments ($n = 6$), group II underwent LFP recording experiments ($n = 6$), group III underwent MUA recording experiments ($n = 3$), group IV underwent rsfMRI experiments ($n = 18$, low-frequency stimulation, $n = 8$, high-frequency stimulation and $n = 12$, TTX infusion), group V underwent LFP recording experiments at resting state ($n = 8$, low-frequency stimulation), and group VI underwent optogenetic vfMRI experiments ($n = 8$). Full details of animal surgical procedures, optogenetic stimulation paradigms, optogenetic fMRI/rsfMRI/vfMRI acquisition and analysis procedures, electrophysiological recordings and analysis protocols, and histology are provided in *SI Methods*.

Data and Code Availability. The data that support the findings of this study and computer codes used are available from the corresponding author upon request.

ACKNOWLEDGMENTS. We thank Drs. I. Timofeev, M. M. Poo, C. S. Poon, J. H. Lee, and X. Han for their insightful comments; Drs. W. H. Yung, K. K. Tsia, Y. I. Shih, Q. Li, S. J. Fan, A. To, and Misters A. Mok and Y. Qui for their technical assistance; and Dr. K. Deisseroth who provided us with the ChR2 viral construct. This work was supported by the Hong Kong Research Grant Council (Grants C7048-16G and HKU17103015 to E.X.W.) and the Lam Woo Foundation.

1. Scoville WB, Milner B (1957) Loss of recent memory after bilateral hippocampal lesions. *J Neurol Neurosurg Psychiatry* 20:11–21.
2. Squire LR (1992) Memory and the hippocampus: A synthesis from findings with rats, monkeys, and humans. *Psychol Rev* 99:195–231.
3. Maguire EA, et al. (1998) Knowing where and getting there: A human navigation network. *Science* 280:921–924.
4. Buzsáki G, Moser EI (2013) Memory, navigation and theta rhythm in the hippocampal-entorhinal system. *Nat Neurosci* 16:130–138.
5. van Strien NM, Cappaert NL, Witter MP (2009) The anatomy of memory: An interactive overview of the parahippocampal-hippocampal network. *Nat Rev Neurosci* 10:272–282.
6. Yeckel MF, Berger TW (1990) Feedforward excitation of the hippocampus by afferents from the entorhinal cortex: Redefinition of the role of the trisynaptic pathway. *Proc Natl Acad Sci USA* 87:5832–5836.
7. Fanselow MS, Dong HW (2010) Are the dorsal and ventral hippocampus functionally distinct structures? *Neuron* 65:7–19.
8. Strange BA, Witter MP, Lein ES, Moser EI (2014) Functional organization of the hippocampal longitudinal axis. *Nat Rev Neurosci* 15:655–669.
9. Ji D, Wilson MA (2007) Coordinated memory replay in the visual cortex and hippocampus during sleep. *Nat Neurosci* 10:100–107.
10. Buzsáki G (1996) The hippocampo-neocortical dialogue. *Cereb Cortex* 6:81–92.
11. Fox MD, Raichle ME (2007) Spontaneous fluctuations in brain activity observed with functional magnetic resonance imaging. *Nat Rev Neurosci* 8:700–711.
12. Smith SM, et al.; WU-Minn HCP Consortium (2013) Resting-state fMRI in the Human Connectome Project. *Neuroimage* 80:144–168.
13. Buckner RL, Krienen FM, Yeo BT (2013) Opportunities and limitations of intrinsic functional connectivity MRI. *Nat Neurosci* 16:832–837.
14. Zhou IY, et al. (2014) Brain resting-state functional MRI connectivity: Morphological foundation and plasticity. *Neuroimage* 84:1–10.
15. Park HJ, Friston K (2013) Structural and functional brain networks: From connections to cognition. *Science* 342:1238411.
16. Lu H, et al. (2016) Low- but not high-frequency LFP correlates with spontaneous BOLD fluctuations in rat whisker barrel cortex. *Cereb Cortex* 26:683–694.
17. Lu H, et al. (2007) Synchronized delta oscillations correlate with the resting-state functional MRI signal. *Proc Natl Acad Sci USA* 104:18265–18269.
18. Wang L, Saalmann YB, Pinsk MA, Arcaro MJ, Kastner S (2012) Electrophysiological low-frequency coherence and cross-frequency coupling contribute to BOLD connectivity. *Neuron* 76:1010–1020.
19. Schölvinck ML, Maier A, Ye FQ, Duyn JH, Leopold DA (2010) Neural basis of global resting-state fMRI activity. *Proc Natl Acad Sci USA* 107:10238–10243.
20. Buzsáki G, Draguhn A (2004) Neuronal oscillations in cortical networks. *Science* 304:1926–1929.
21. Sheroziya M, Timofeev I (2014) Global intracellular slow-wave dynamics of the thalamocortical system. *J Neurosci* 34:8875–8893.
22. Matsui T, Murakami T, Ohki K (2016) Transient neuronal coactivations embedded in globally propagating waves underlie resting-state functional connectivity. *Proc Natl Acad Sci USA* 113:6556–6561.
23. Amemiya S, Takao H, Hanaoka S, Ohtomo K (2016) Global and structured waves of rs-fMRI signal identified as putative propagation of spontaneous neural activity. *Neuroimage* 133:331–340.

24. Mitra A, Snyder AZ, Tagliazucchi E, Laufs H, Raichle ME (2015) Propagated infra-slow intrinsic brain activity reorganizes across wake and slow wave sleep. *Elife* 4:e10781.
25. Ma Y, et al. (2016) Resting-state hemodynamics are spatiotemporally coupled to synchronized and symmetric neural activity in excitatory neurons. *Proc Natl Acad Sci USA* 113:E8463–E8471.
26. Steriade M, Nuñez A, Amzica F (1993) A novel slow (< 1 Hz) oscillation of neocortical neurons in vivo: Depolarizing and hyperpolarizing components. *J Neurosci* 13: 3252–3265.
27. Volgushev M, Chauvette S, Mukovski M, Timofeev I (2006) Precise long-range synchronization of activity and silence in neocortical neurons during slow-wave oscillations [corrected]. *J Neurosci* 26:5665–5672, and erratum (2006) 26.
28. Chauvette S, Crochet S, Volgushev M, Timofeev I (2011) Properties of slow oscillation during slow-wave sleep and anesthesia in cats. *J Neurosci* 31:14998–15008.
29. Neske GT (2016) The slow oscillation in cortical and thalamic networks: Mechanisms and functions. *Front Neural Circuits* 9:88.
30. Wolansky T, Clement EA, Peters SR, Palczak MA, Dickson CT (2006) Hippocampal slow oscillation: A novel EEG state and its coordination with ongoing neocortical activity. *J Neurosci* 26:6213–6229.
31. Hahn TT, Sakmann B, Mehta MR (2007) Differential responses of hippocampal subfields to cortical up-down states. *Proc Natl Acad Sci USA* 104:5169–5174.
32. Cole MW, Pathak S, Schneider W (2010) Identifying the brain's most globally connected regions. *Neuroimage* 49:3132–3148.
33. Power JD, Schlaggar BL, Lessov-Schlaggar CN, Petersen SE (2013) Evidence for hubs in human functional brain networks. *Neuron* 79:798–813.
34. Mitra A, et al. (2016) Human cortical-hippocampal dialogue in wake and slow-wave sleep. *Proc Natl Acad Sci USA* 113:E6868–E6876.
35. Lee JH, et al. (2010) Global and local fMRI signals driven by neurons defined optogenetically by type and wiring. *Nature* 465:788–792.
36. Leong AT, et al. (2016) Long-range projections coordinate distributed brain-wide neural activity with a specific spatiotemporal profile. *Proc Natl Acad Sci USA* 113: E8306–E8315.
37. Ferenczi EA, et al. (2016) Prefrontal cortical regulation of brainwide circuit dynamics and reward-related behavior. *Science* 351:aac9698.
38. Yu X, et al. (2016) Sensory and optogenetically driven single-vessel fMRI. *Nat Methods* 13:337–340.
39. Logothetis NK, Pauls J, Augath M, Trinath T, Oeltermann A (2001) Neurophysiological investigation of the basis of the fMRI signal. *Nature* 412:150–157.
40. Boudkkazi S, et al. (2007) Release-dependent variations in synaptic latency: A putative code for short- and long-term synaptic dynamics. *Neuron* 56:1048–1060.
41. Canolty RT, Knight RT (2010) The functional role of cross-frequency coupling. *Trends Cogn Sci* 14:506–515.
42. Preston AR, Eichenbaum H (2013) Interplay of hippocampus and prefrontal cortex in memory. *Curr Biol* 23:R764–R773.
43. Brincat SL, Miller EK (2015) Frequency-specific hippocampal-prefrontal interactions during associative learning. *Nat Neurosci* 18:576–581.
44. Logothetis NK (2015) Neural-event-triggered fMRI of large-scale neural networks. *Curr Opin Neurobiol* 31:214–222.
45. Ramirez-Villegas JF, Logothetis NK, Besserve M (2015) Diversity of sharp-wave-ripple LFP signatures reveals differentiated brain-wide dynamical events. *Proc Natl Acad Sci USA* 112:E6379–E6387.
46. Logothetis NK, et al. (2012) Hippocampal-cortical interaction during periods of subcortical silence. *Nature* 491:547–553.
47. Staresina BP, et al. (2015) Hierarchical nesting of slow oscillations, spindles and ripples in the human hippocampus during sleep. *Nat Neurosci* 18:1679–1686.
48. Mölle M, Yeshenko O, Marshall L, Sara SJ, Born J (2006) Hippocampal sharp wave-ripples linked to slow oscillations in rat slow-wave sleep. *J Neurophysiol* 96:62–70.
49. Sirota A, Csicsvari J, Buhl D, Buzsáki G (2003) Communication between neocortex and hippocampus during sleep in rodents. *Proc Natl Acad Sci USA* 100:2065–2069.
50. Siapas AG, Wilson MA (1998) Coordinated interactions between hippocampal ripples and cortical spindles during slow-wave sleep. *Neuron* 21:1123–1128.
51. Crunelli V, David F, Lőrincz ML, Hughes SW (2015) The thalamocortical network as a single slow wave-generating unit. *Curr Opin Neurobiol* 31:72–80.
52. Crunelli V, Hughes SW (2010) The slow (<1 Hz) rhythm of non-REM sleep: A dialogue between three cardinal oscillators. *Nat Neurosci* 13:9–17.
53. Steriade M, McCormick DA, Sejnowski TJ (1993) Thalamocortical oscillations in the sleeping and aroused brain. *Science* 262:679–685.
54. Xiao D, et al. (2017) Mapping cortical mesoscopic networks of single spiking cortical or sub-cortical neurons. *Elife* 6:e19976.
55. Mohajerani MH, et al. (2013) Spontaneous cortical activity alternates between motifs defined by regional axonal projections. *Nat Neurosci* 16:1426–1435.
56. Martínez-García F, González-Hernández T, Martínez-Millán L (1994) Pyramidal and nonpyramidal callosal cells in the striate cortex of the adult rat. *J Comp Neurol* 350: 439–451.
57. Moreno A, Morris RGM, Canals S (2016) Frequency-dependent gating of hippocampal-neocortical interactions. *Cereb Cortex* 26:2105–2114.
58. Weitz AJ, et al. (2015) Optogenetic fMRI reveals distinct, frequency-dependent networks recruited by dorsal and intermediate hippocampus stimulations. *Neuroimage* 107:229–241.
59. He BJ, Snyder AZ, Zempel JM, Smyth MD, Raichle ME (2008) Electrophysiological correlates of the brain's intrinsic large-scale functional architecture. *Proc Natl Acad Sci USA* 105:16039–16044.
60. Colgin LL (2016) Rhythms of the hippocampal network. *Nat Rev Neurosci* 17:239–249.
61. Jutras MJ, Fries P, Buffalo EA (2013) Oscillatory activity in the monkey hippocampus during visual exploration and memory formation. *Proc Natl Acad Sci USA* 110: 13144–13149.
62. Wang Y, Romani S, Lustig B, Leonardo A, Pastalkova E (2015) Theta sequences are essential for internally generated hippocampal firing fields. *Nat Neurosci* 18:282–288.
63. Siegle JH, Wilson MA (2014) Enhancement of encoding and retrieval functions through theta phase-specific manipulation of hippocampus. *Elife* 3:e03061.
64. Vass LK, et al. (2016) Oscillations go the distance: Low-frequency human hippocampal oscillations code spatial distance in the absence of sensory cues during teleportation. *Neuron* 89:1180–1186.
65. Jacobs J (2013) Hippocampal theta oscillations are slower in humans than in rodents: Implications for models of spatial navigation and memory. *Philos Trans R Soc Lond B Biol Sci* 369:20130304.
66. Perouansky M, et al. (2010) Slowing of the hippocampal θ rhythm correlates with anesthetic-induced amnesia. *Anesthesiology* 113:1299–1309.
67. Lustig B, Wang Y, Pastalkova E (2016) Oscillatory patterns in hippocampus under light and deep isoflurane anesthesia closely mirror prominent brain states in awake animals. *Hippocampus* 26:102–109.
68. Pawela CP, et al. (2008) Resting-state functional connectivity of the rat brain. *Magn Reson Med* 59:1021–1029.
69. Zhou ZC, et al. (2016) Resting state network topology of the ferret brain. *Neuroimage* 143:70–81.
70. Belcher AM, et al. (2016) Functional connectivity hubs and networks in the awake marmoset brain. *Front Integr Nuerosci* 10:9.
71. Vincent JL, et al. (2007) Intrinsic functional architecture in the anaesthetized monkey brain. *Nature* 447:83–86.
72. Larson-Prior LJ, et al. (2009) Cortical network functional connectivity in the descent to sleep. *Proc Natl Acad Sci USA* 106:4489–4494.
73. Damoiseaux JS, et al. (2006) Consistent resting-state networks across healthy subjects. *Proc Natl Acad Sci USA* 103:13848–13853.
74. Lu H, et al. (2012) Rat brains also have a default mode network. *Proc Natl Acad Sci USA* 109:3979–3984.
75. McCormick DA, et al. (2003) Persistent cortical activity: Mechanisms of generation and effects on neuronal excitability. *Cereb Cortex* 13:1219–1231.
76. Shu Y, Hasenstaub A, Badoual M, Bal T, McCormick DA (2003) Barrages of synaptic activity control the gain and sensitivity of cortical neurons. *J Neurosci* 23: 10388–10401.
77. Arieli A, Sterkin A, Grinvald A, Aertsen A (1996) Dynamics of ongoing activity: Explanation of the large variability in evoked cortical responses. *Science* 273:1868–1871.
78. Haider B, Duque A, Hasenstaub AR, Yu Y, McCormick DA (2007) Enhancement of visual responsiveness by spontaneous local network activity in vivo. *J Neurophysiol* 97: 4186–4202.
79. Pilz GA, et al. (2016) Functional imaging of dentate granule cells in the adult mouse hippocampus. *J Neurosci* 36:7407–7414.
80. Brown EN, Lydic R, Schiff ND (2010) General anesthesia, sleep, and coma. *N Engl J Med* 363:2638–2650.
81. Li CY, Poo MM, Dan Y (2009) Burst spiking of a single cortical neuron modifies global brain state. *Science* 324:643–646.
82. Sharma AV, Wolansky T, Dickson CT (2010) A comparison of sleeplike slow oscillations in the hippocampus under ketamine and urethane anesthesia. *J Neurophysiol* 104: 932–939.
83. Telensky P, et al. (2011) Functional inactivation of the rat hippocampus disrupts avoidance of a moving object. *Proc Natl Acad Sci USA* 108:5414–5418.
84. Gao PP, Zhang JW, Fan SJ, Sanes DH, Wu EX (2015) Auditory midbrain processing is differentially modulated by auditory and visual cortices: An auditory fMRI study. *Neuroimage* 123:22–32.
85. Herman AM, Huang L, Murphey DK, Garcia I, Arenkiel BR (2014) Cell type-specific and time-dependent light exposure contribute to silencing in neurons expressing Channelrhodopsin-2. *Elife* 3:e01481.
86. Li JM, Bentley WJ, Snyder LH (2015) Functional connectivity arises from a slow rhythmic mechanism. *Proc Natl Acad Sci USA* 112:E2527–E2535, and correction (2015) 112:E5221.
87. Sparta DR, et al. (2011) Construction of implantable optical fibers for long-term optogenetic manipulation of neural circuits. *Nat Protoc* 7:12–23.